Metallacarboranes in Catalysis. 7. Kinetics and Mechanism of Acrylate Ester Hydrogenation Catalyzed by *closo*-Rhodacarboranes[1]

Paul E. Behnken,[2] David C. Busby, Mark S. Delaney, Roswell E. King III, Charles W. Kreimendahl,[3a] Todd B. Marder,[3b] Joseph J. Wilczynski, and M. Frederick Hawthorne*

Contribution from the Department of Chemistry and Biochemistry, University of California, Los Angeles, California 90024. *Received January 13, 1984*

Abstract: In a search for reactions catalyzed by rhodacarborane clusters, the species I, [*closo*-3,3-$(PPh_3)_2$-3-H-3,1,2-$RhC_2B_9H_{11}$], II, [*closo*-2,2-$(PPh_3)_2$-2-H-2,1,7-$RhC_2B_9H_{11}$], III, [*closo*-2,2-$(PPh_3)_2$-2-H-2,1,12-$RhC_2B_9H_{11}$], and IV, [*exo-nido*-$(PPh_3)_2$Rh-μ-7,8-$(CH_2)_3$-7,8-$C_2B_9H_{10}$], were examined as catalyst precursors in the hydrogenation of 1-butyl acrylate (C) in THF solution at 40.8 °C. Only catalyst precursors I and III gave results that were free of complications and suitable for detailed kinetic analyses. Both I and III reversibly hydridometalate C to produce the chelated closo adducts VI and VII, respectively, and an equivalent quantity of PPh_3. The slow attainment of equilibria in these hydridometalation reactions accounts for the appearance of a lengthy induction period at the outset of C hydrogenations which employed either I or III as catalyst precursor. The rate law for C hydrogenation using I or III was elucidated and found to be identical in form with that previously observed using *closo*- or *exo-nido*-rhodacarboranes in 3-methyl-3-phenylbutene-1 (A) hydrogenation. As in the case of A, it was shown by deuterium labeling that C hydrogenation did not involve the hydride ligand at the RhH vertex of either I of III. The BH vertices of these same species were similarly shown to not be involved. Reduction of C with D_2 using I as the catalyst source gave a moderate amount of D scrambling into recovered C and produced 1-butyl propionate-d_0-d_4. The above results led to a proposed catalytic cycle that culminates in the slow, but probably not rate-limiting, elimination of 1-butyl propionate from a reversibly formed exo-nido alkyl hydride intermediate. These kinetic characteristics may have their origin in the weak electron donor properties of the chelated [*exo-nido*-$C_2B_9H_{12}$]$^-$ ligands that are attached to Rh(1+) or Rh(3+) in exo-nido intermediates by a pair of B-H-Rh three-center bonds.

The previous paper of this series[4] described a search for cluster catalysis mechanisms using rhodacarboranes as catalyst precursors in conjunction with 3-methyl-3-phenyl-1-butene (A) hydrogenation and 1-hexene (B) isomerization and hydrogenation reactions. This paper describes additional mechanism studies that employed *closo*-bis(triphenylphosphine)hydridorhodacarboranes[5] as catalyst precursors in the hydrogenation of the representative acrylate ester, 1-butyl acrylate (C). The rhodacarboranes [*closo*-3,3-$(PPh_3)_2$-3-H-3,1,2-$RhC_2B_9H_{11}$] (I),[5] [*closo*-2,2-$(PPh_3)_2$-2-H-2,1,7-$RhC_2B_9H_{11}$] (II),[5] [*closo*-2,2-$(PPh_3)_2$-2-H-2,1,12-$RhC_2B_9H_{11}$] (III),[5] and [*exo-nido*-$(PPh_3)_2$Rh-μ-7,8-$(CH_2)_3$-7,8-$C_2B_9H_{10}$] (IV)[6] were examined in the hydrogenation of C, but due to experimental limitations only precursors I and III were studied in detail. As will be shown below, the general mechanism of hydrogenation of an alkene carrying a conjugated electron-withdrawing C(O)OR substituent does not markedly differ from the general mechanism proposed for A and B hydrogenation with catalyst precursors I-IV. The unusual mechanistic feature that has been found to characterize all rhodacarborane-catalyzed hydrogenation reactions[4] studied thus far is the very facile reversibility of HRh^{III}(alkyl) formation and the relative slowness with which this intermediate reductively eliminates alkane. Evidence for this marked reversibility came from the observed distribution of deuterium between alkene and alkane in alkene reductions carried out with D_2 and catalyst precursors I-IV.[4] In addition, the reduction of 1-hexene with D_2 using the exo-nido catalyst precursor IV the deuterium balance parameter,[4] Δ, was found to be near 1.6. This fact proved that 60% more deuterium than that required for the formation of product alkane had entered the alkene-alkane species present. This clearly suggested[4] reversibility of the entire hydrogenation sequence from hydridorhodium alkyl to component alkene and H_2. In other cases, Δ varied from 0.9 to 1.1 with some inherent error. Consequently, the proposal was made[4] that decomposition of HRh^{III}(alkyl) to form alkane was rate determining at moderate H_2 pressures since the [*exo-nido*-$C_2B_9H_{12}$]$^-$ family of ligands would be expected to have very poor electron-donating properties and provide a very small trans effect (influence) and correspondingly reduced driving force for the reductive elimination of alkane.[4] An alternative explanation will be developed here that suggests rate-determining activation of H_2 followed by a series of rapid and reversible steps which account for D scrambling as previously described[4] and culminates in the slower reductive elimination of alkane from HRh^{III}(alkyl). The overall rate law does not distinguish between these two possibilities.

The observation of equilibria unrelated to hydrogenation that involve the reversible formation of chelated closo-acrylate ester-hydridorhodacarborane adducts serves to further emphasize the importance of closo-exo-nido tautomerism[6] in certain rhodacarborane-catalyzed reactions and complements our previously reported studies.[4,7a] In addition, the slow and reversible formation of the acrylate adducts results in a lengthy induction period for hydrogenation that is terminated only after the equilibrium concentration of adduct is attained.

Results

The selection of C as the substrate for these hydrogenation studies was suggested by its low volatility, ease of purification, and initial studies which proved that C would provide reproducible hydrogenation rates using catalyst precursors I and III. The use

(1) Taken in part from the Ph.D. Thesis of Roswell E. King, University of California, Los Angeles, 1982.
(2) University of California Regents' Fellow, 1979-1980.
(3) (a) University Fellow, 1981. (b) University of California Regents' Intern Fellow, 1976-1980.
(4) Behnken, P. E.; Belmont, J. A.; Busby, D. C.; Delaney, M. S.; King, R. E., III; Kreimendahl, C. W.; Marder, T. B.; Wilczynski, J. J.; Hawthorne, M. F. *J. Am. Chem. Soc.* **1984**, *106*, 3011.
(5) Baker, R. T.; Delaney, M. S.; King, R. E., III, Knobler, C. B.; Long, J. A.; Marder, T. B.; Paxson, T. E.; Teller, R. G.; Hawthorne, M. F. *J. Am. Chem. Soc.* **1984**, *106*, 2965.
(6) Long, J. A.; Marder, T. B.; Behnken, P. E.; Hawthorne, M. F. *J. Am. Chem. Soc.* **1984**, *106*, 2979.
(7) (a) Long, J. A.; Marder, T. B.; Hawthorne, M. F. *J. Am. Chem. Soc.* **1984**, *106*, 3004. (b) Hewes, J. D.; Kreimendahl, C. W.; Marder, T. B.; Hawthorne, M. F. *J. Am. Chem. Soc.* **1984**, *106*, 5757.

0002-7863/84/1506-7444$01.50/0

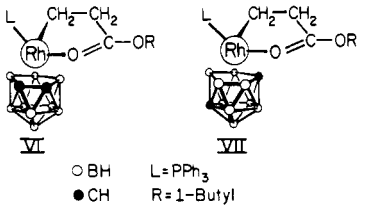

Figure 1. Structures of 1-butyl acrylate hydridometalation adducts VI and VII derived from catalyst precursors I and III, respectively.

of precursor II gave erratic reaction rates as previously observed using A as the hydrogenation substrate.[4] The exo-nido precursor IV was rapidly converted to a species believed to be the corresponding chelated *closo*-acrylate–hydridorhodacarborane adduct (vide infra) and then irreversibly diverted to a novel hydroboration product that was described elsewhere.[7b] In view of these results, only catalyst precursors I and III were subjected to kinetic studies.

Chelated *closo*-Acrylate Ester–Hydridorhodacarborane Adducts. In a previous paper[5] of this series we described the reversible insertion of acrylate, methacrylate, and atropate esters into the RhH vertex of a *closo*-hydridobis(triphenylphosphine)-rhodacarborane accompanied by loss of PPh_3 from Rh and chelation of the ester carbonyl oxygen atom to the Rh (3+) vertex. As an example, the chelated closo-alkyl derivative V generated from [*d-closo*-1-Me-3,3-$(PPh_3)_2$-3-H-3,1,2-$RhC_2B_9H_{10}$] and 1-butyl acrylate was the subject of an X-ray diffraction study[5] that provided the structure and absolute configuration of one diastereoisomer of V. The generality of these reversible hydridometalation reactions suggested that I and III should react with C in this manner to form the chelated alkyl adducts VI and VII, respectively. Indeed, the kinetic experiments described below and the associated rate law demanded that VI and VII be generated reversibly during hydrogenation reactions.

Mixing tetrahydrofuran (THF) solutions of C with similar solutions of I or III at 41 °C resulted in a slow deepening of the characteristic yellow color of the rhodium complexes and the formation of the corresponding chelates. Equation 1 defines the

$$\text{I} + \text{C} \overset{K_{VI}}{\rightleftharpoons} \text{VI} + PPh_3 \qquad (1)$$

$$\text{III} + \text{C} \overset{K_{VII}}{\rightleftharpoons} \text{VII} + PPh_3$$

equilibria involved in these reactions. The complexes VI and VII were easily recognized by comparison of the $^{31}P\{^1H\}$ FT NMR of equilibrated samples prepared in situ in THF (10% benzene-d_6) at 41 °C with that of V: VI, d, 38.1 ppm, J_{Rh-P} = 140 Hz; VII, d, 31.7 ppm, J_{Rh-P} = 112 Hz; V, d, 31.7 ppm, J_{Rh-P} = 139 Hz. In another experiment a solution of I containing excess methyl acrylate (mole ratio 1:30) was equilibrated at 41 °C until ca. 30% chelated alkyl complex had been formed; $^{31}P\{^1H\}$, d, +38.2, J_{Rh-P} = 139 Hz. The 200-MHz ^1H FT NMR of this sample at low temperatures revealed no resonances that could be assigned to B–H–B or Rh–H–B bridge protons characteristic of exo-nido complexes. In addition, the ^{11}B NMR spectrum of this same sample contained no upfield resonances (ca. −35 ppm) characteristic[6] of *exo-nido*-rhodacarboranes. Since the $^{31}P\{^1H\}$ spectra of VI and VII could be distinguished in the presence of I and III, respectively (I, d, 39.7, J_{Rh-P} = 125 Hz; III, d, 35.5, J_{Rh-P} = 111 Hz), it was possible to estimate the values of the equilibrium constants K_{VI} and K_{VII} (eq 1) in THF at 41 °C by integration of the $^{31}P\{^1H\}$ spectra of equilibrated solutions of C with I or III. The values of K_{VI} and K_{VII} were approximately 1×10^{-3} and 1×10^{-2}, respectively. Attempts to estimate the equilibrium constant for the reaction of C with II were unsuccessful due to overlap of the ^{31}P resonances of II and its chelated complex.

The reactions of C with I and III to form VI and VII, respectively, were quite slow, and 8–10 h were required at 41 °C in order to achieve equilibration. Related to these observations is the fact that the RhD vertex present in I-*3-d* exchanges with CH in C, presumably through the reversible formation of VI, at a very low initial rate at 41 °C in THF ($k = 1.4 \times 10^{-6}$ s^{-1} with $[C]_0$ = 0.16 M). Reactions of this sort were followed by integration of the developing RhH resonance using ^1H FT NMR. Since it is quite clear that VI is reversibly formed from I and C, albeit at a low rate, the extremely slow RhD exchange with C strongly suggests that the D atom in question may, to a large extent, be stereospecifically and reversibly transferred between rhodium and the chiral CHDCOOR center present in VI.[5] Such a process, if stereochemically rigorous, would prevent mixing of the H and D atoms at the chiral carbon atom in VI.[5] Further discussion of these possibilities will be deferred until additional experimental evidence is accumulated.

Deuterium Labeling Experiments. In order to evaluate the integrity of B–D labels attached to I during the hydrogenation of C the catalyst precursor [*closo*-3,3-$(PPh_3)_2$-3-H-3,1,2-Rh-$(C_2H_2)(B_9D_9)$] (I-d_9)[4] was employed in the hydrogenation of C under the conditions normally employed in kientic experiments (vide infra). After 90 catalyst turnovers the ^{11}B FT NMR spectrum of recovered catalyst precursor contained no evidence of $^{11}B-^1H$ coupling, thereby proving that B–D (B–H) bonds are not involved in hydrogenation or related processes. An identical result was previously observed during A hydrogenation.[4]

The fate of the RhD vertex in I-*3-d*[4,5] was examined in two rate runs that were carried to partial completion with 0.58 atm of H_2 under the usual hydrogenation reaction conditions. After seven hydrogenation turnovers the recovered catalyst precursor had retained 84% of its original (95%) RhD content, and in the second rate run 74% of the original RhD was present after 11 turnovers. In these experiments the ^1H FT NMR spectrum of I was monitored in the RhH region. These results conclusively prove that C, as in the case of A,[4] is hydrogenated in a mechanism that does not involve direct utilization of the hydride ligand attached to Rh. The slow loss of the D label from I-*3-d* in these reactions may occur through the same very slow process seen in the D exchange of I-*3-d* with C in the absence of H_2, which was described above.

Hydrogenation of 1-Butyl Acrylate (C) with the Catalyst Precursors I and III. As inferred above, preliminary experiments proved that C could be hydrogenated by using catalyst precursors I and III without problems of poor reproducibility from run to run or between different preparations of I or III. As expected, 1-butyl propionate was the only organic product of these reactions and the I or III employed in each experiment could be recovered in essentially quantitative yield following the completion of the reaction. All kinetic experiments were conducted at 40.8 °C in THF and in the absence of added PPh_3. When added, PPh_3 depressed the hydrogenation rates to the extent that reactions become prohibitively slow. The initial C concentration in all rate runs was 0.18 M, and the concentration of I or III was varied over a wide range. Hydrogen partial pressure was constant throughout each rate run and was varied between 0.15 and 1.5 atm (2.5×10^{-4} and 2.5×10^{-3} M at 40.8 °C)[8] by using the automatic hydrogen titrator previously described.

The hydrogenation of C using I or III was characterized by a lengthy induction period that, as will be shown below, is due to the slow formation of VI or VII and an equivalent quantity of PPh_3. The induction period could be eliminated by an 8-h preequilibration of C with I or III in the absence of H_2. Under certain conditions, the induction period was sufficiently long to allow the consumption of as much as 40% of the C initially present before the steady state was reached. Low H_2 pressures reduced the quantity of C consumed in this manner and increased the length of the induction period while higher H_2 pressures gave opposite effects.[9] Following the induction period, each kinetic run became half-order in C with an observed rate constant, k_{obsd}, which was itself half-order in added I or III, $[Rh]_t$. All rate data

(8) The solubility of H_2 in tetrahydrofuran at 40.8 °C is $(1.7 \pm 0.1) \times 10^{-3}$ M atm^{-1}. We are indebted to Prof. Brian James for this measurement.

(9) At high H_2 pressures the [C] approaches a lower steady-state value seen at the end of the induction period through the operation of two processes that comsume C; hydrogenation and the reversible formation of VI. At lower H_2 pressures the former process makes a much less important contribution to the consumption of [C] and the relatively slow formation of significantly more VI is required to reach initial equilibrium beween C and VI. Consequently, the apparent induction period is longer at low H_2 pressures.

Table I. Collected Rate Data for the Hydrogenation of 0.18 M 1-Butyl Acrylate Using Catalyst Precursors I and III in THF at 40.8 °C

cat. precursor	[precursor]	$[H_2]^a$	k_{obsd}, $M^{-1/2}$ s^{-1}	k'_{corr}, s^{-1}
I	2.00×10^{-2}	9.86×10^{-4}	3.12×10^{-5}	7.14×10^{-6} [b]
	1.61×10^{-2}	9.86×10^{-4}	2.94×10^{-5}	7.51×10^{-6} [b]
	1.53×10^{-2}	9.86×10^{-4}	2.85×10^{-5}	7.46×10^{-6} [b]
	8.03×10^{-3}	9.86×10^{-4}	2.04×10^{-5}	7.46×10^{-6} [b]
	4.01×10^{-3}	9.86×10^{-4}	1.42×10^{-5}	7.46×10^{-6} [b]
	2.00×10^{-2}	9.86×10^{-4}	3.05×10^{-5}	6.98×10^{-6} [b]
	2.00×10^{-2}	2.53×10^{-4}	1.10×10^{-5}	2.51×10^{-6}
	2.00×10^{-2}	4.58×10^{-4}	1.83×10^{-5}	4.18×10^{-6}
	2.00×10^{-2}	1.97×10^{-3}	4.62×10^{-5}	1.06×10^{-5}
	1.50×10^{-2}	2.46×10^{-3}	4.67×10^{-5}	1.24×10^{-5}
III	4.98×10^{-3}	2.45×10^{-3}	3.05×10^{-5}	5.01×10^{-5}
	4.87×10^{-3}	1.48×10^{-3}	2.15×10^{-5}	3.65×10^{-5}
	1.54×10^{-2}	9.86×10^{-4}	2.86×10^{-5}	2.48×10^{-5}
	5.13×10^{-3}	4.54×10^{-4}	8.07×10^{-6}	1.27×10^{-5}

[a] Solubility of H_2 in THF at 41 °C is 1.7×10^{-3} M atm^{-1}. [b] Averaged with five other values determined at this $[H_2]$ to give plotted (Figure 3) value 7.34×10^{-6} s^{-1}.

were treated by using the appropriate half-order integrated equation to generate k_{obsd} values.

The reproducibility of rate constants, k, was in all cases approximately ±3% at a constant H_2 pressure in accord with eq 2, where $[I]_0$ or $[III]_0 = [Rh]_t$, the total Rh concentration.

$$\frac{-d[H_2]}{dt} = k[(C)]^{1/2}[Rh]_t^{1/2} \qquad (2)$$

The induction periods observed in all rate runs conducted in the absence of preequilibration coincided with the accumulation of VI or VII and PPh_3 (vide infra) through the K_{VI} or K_{VII} equilibria of eq 1. This fact, coupled with the demonstrated lack of direct involvement of the hydride ligand attached to Rh in I during hydrogenation, suggests that VI (and by inference VII) does not lie upon the hydrogenation reaction coordinate, but instead it affects the reaction rates (induction period, etc.) by being directly accessible from an intermediate necessary for hydrogenation. Thus, VI or VII, as the case may be, accumulates during the induction period, and, after steady-state concentrations of VI or VII and PPh_3 are established, it is the liberated PPh_3 that is indirectly seen in the $[C]^{1/2}$ and $[Rh]_t^{1/2}$ terms of the experimental rate equation. Thus, the rate expression (2) may be rewritten as eq 3 in accord with the corresponding rate expression observed

$$\frac{-d[H_2]}{dt} = \frac{k'[(C)][Rh]_t}{[PPh_3]} = \frac{k'[(C)][Rh]_t}{(K_{VI}[(C)][Rh]_t)^{1/2}} = k[(C)]^{1/2}[Rh]_t^{1/2} \qquad (3)$$

in A hydrogenation since $[PPh_3] \simeq (K_{VI}[C][I]_0)^{1/2}$ or $(K_{VII}[C][III]_0)^{1/2}$. While the relationships of eq 2 and 3 link the observed rate data with the previously reported rate law for A hydrogenation,[4] they do not yield quantitatively precise values for k. This lack of precision is due to the fact that eq 2 and 3 ignore the fact that $[I]_0$ is not the instantaneous [I] following the induction period, since a few percent of I has been converted to complex VI and PPh_3. Since K_{VI} is known to be ca. 10^{-3}, it follows that a more precise value of k' can be calculated by using eq 4 where $[PPh_3] = [VI]$.

$$\frac{-d[H_2]}{dt} = \frac{k'_{corr}([I]_0 - [VI])[(C)]}{[PPh_3]} \qquad (4)$$

This inadequacy of eq 3 is even greater in the case of precursor III since $K_{VII} = 10^{-2}$, and an even greater proportion of $[III]_0$ is converted to complex VII. In order to obtain as accurate rate data as possible for the evaluation of the dependence of rate upon $[H_2]$, k'_{corr} was calculated for each rate run at 75% reaction ($[C] = 4.5 \times 10^{-2}$ M) using eq 4, the experimental rate, $-d[H_2]/dt = k_{obsd}[C]^{1/2}$, and $[PPh_3] = [VI]$ (or VII in the case of precursor III) derived from the equilibria (eq 1) and the known values of K_{VI} (or K_{VII}). Table I presents hydrogenation rate data collected at a variety of hydrogen pressures using I and III from which the empirical relationship of rate vs. $[H_2]$ was derived (eq 5). Just

$$1/k'_{corr} = \frac{m}{[H_2]} + C \quad \text{and} \quad k'_{corr} = \frac{[H_2]}{m + C[H_2]} \qquad (5)$$

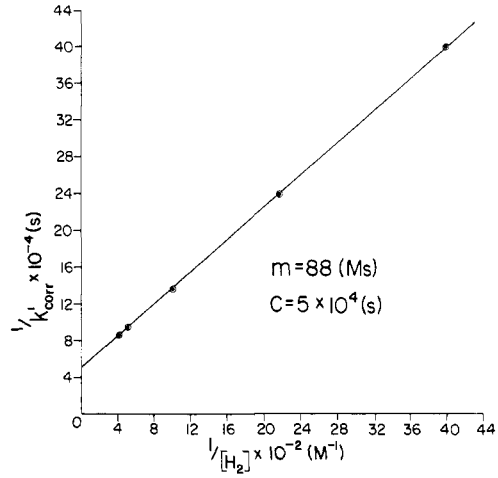

Figure 2. Plot of $(k'_{corr})^{-1}$ vs. $[H_2]^{-1}$ using catalyst precursor I.

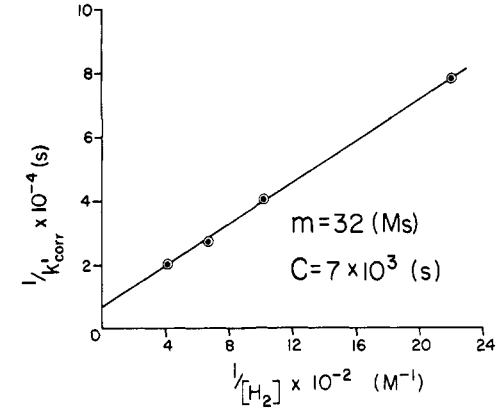

Figure 3. Plot of $(k'_{corr})^{-1}$ vs. $[H_2]^{-1}$ using catalyst precursor III.

as in the case of A hydrogenation catalyzed by I,[4] plots of $(k'_{corr})^{-1}$ vs. $[H_2]^{-1}$ were linear with the following slopes and intercepts for I and III, respectively: $m^I = 88$ Ms, $C^I = 5.0 \times 10^4$ s, $m^{III} = 32$ Ms, and $C^{III} = 7.0 \times 10^3$ s. Figures 2 and 3 are $(k'_{corr})^{-1}$ vs. $[H_2]^{-1}$ plots for I and III, respectively. Equation 6 delineates the overall

$$\frac{-d[H_2]}{dt} = \frac{([Rh]_t - [Complex])[(C)][H_2]}{[PPh_3](m + C[H_2])} \qquad (6)$$

rate law derived from eq 4 and 5 where [complex] = [VI] or [VII] = $[PPh_3]$. Expressed in this manner, eq 6 is identical in form with the overall rate law observed in A[4] hydrogenation with I, III, and IV except that in those cases complexes analogous to VI and VII did not exist and [catalyst precursor] $\simeq [Rh]_t$.

Table II. Isotopic Analyses during the Reduction of 0.55 M 1-Butyl Acrylate with 9.9×10^{-3} M Deuterium and 3.9×10^{-3} M I in THF at 40.8 °C

% reaction	cat. turnovers	1-butyl acrylate anal., %			1-butyl propionate anal., %					
		d_0	d_1	d_2	d_0	d_1	d_2	d_3	d_4	Δ^a
3	4	98	1	1	10	26	68			1.33
7	10	98	1	1	4	18	77			1.07
12	17	96	3	1	3	23	70	2	2	1.08
19	27	95	5	1	4	26	64	5	1	0.97
33	46	93	6	1	2	28	61	7	1	0.95
46	64	88	10	2	2	28	60	8	1	0.98
65	91	80	16	4	1	12	83	3	1	1.01

$^a \Delta = \{\sum_{n=1}^{n=3} n[\text{acrylate-}d_n] + \sum_{n=1}^{n=5} n[\text{propionate-}d_n]\}/2\sum_{n=0}^{n=5}[\text{propionate-}d_n] = 1.00$ if no extraneous external exchange of D_2 with CH occurs. See ref 4.

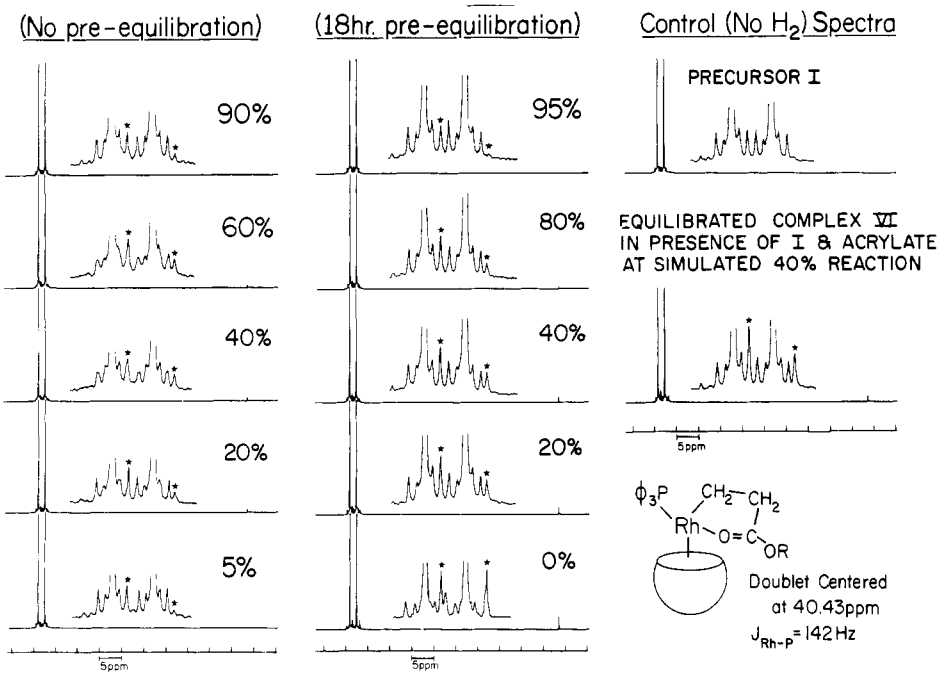

Figure 4. Demonstration of the reversible formation of VI during a hydrogenation experiment by direct observation of VI in the presence of I and PPh_3 using 81.02-MHz $^{31}P\{^1H\}$ FT NMR. Initial concentrations are 0.18 M C and 2×10^{-2} M I. Insets are expanded presentations of spectral regions containing resonances I and VI. Starred resonances arise from complex VI. Percentages refer to percent reaction of C. Control experiments contain 2×10^{-2} M I.

The substitution of D_2 for H_2 at 0.58 atm (9.9×10^{-4} M H_2) in the reduction of C using I produced a small inverse isotope effect, $(k'_{corr})_{H_2}/(k'_{corr})_{D_2}$, of 0.92 in otherwise identical rate runs carried out under the usual conditions.

The effect of the presence of 0.08 M $Cs^+[nido\text{-}7,8\text{-}C_2B_9H_{12}]^-$ upon the rate of hydrogenation of C with 0.02 M I using 9.9×10^{-4} M H_2 and otherwise normal conditions produced a rate dimunition of 13% ($k_{obsd} = 2.7 \times 10^{-5}$ $M^{-1/2}$ s^{-1}) when compared to an identical rate run carried out in the absence of added $[nido\text{-}7,8\text{-}C_2B_9H_{12}]^-$ ($k_{obsd} = 3.1 \times 10^{-5}$ $M^{-1/2}$ s^{-1}). This relatively small rate change does not reasonably appear to be due to the repression of an equilibrium containing $[nido\text{-}7,8\text{-}C_2B_9H_{12}]^-$ as a common ion.

The products of the reaction of C with D_2 (0.58 atm) in the presence of I and in the flow system employed in similar experiments[4] with A and B were studied as a function of time. Table II contains the isotopic distribution of the recovered C and the 1-butyl propionate present at various points in the reaction. The $[C]_0$ was 0.55 M and $[I]_0 = 3.9 \times 10^{-3}$ M, making each percent reaction equivalent to 1.4 turnovers of total Rh. Distribution of deuterium between C and 1-butyl propionate is evident and the D balance parameter, Δ,[4] is essentially unity. The latter fact proves that each mole of D_2 that entered the acrylate or propionate during the reaction was accompanied by the conversion of 1 mol of acrylate to propionate.

Demonstration of the Reversible Formation of VI during the Hydrogenation of C with I. The ability to distinguish relatively low concentrations of VI in the presence of I using $^{31}P\{^1H\}$ FT NMR allowed the formation and subsequent decomposition of VI to be followed throughout hydrogenation reactions carried out under kinetic conditions. Two sets of reactions were carried out at 40.8 °C (1) with no preequilibration of I with C and (2) with an 18-h preequilibration period of I with C. In both cases the $[I]_0$ was 1.5×10^{-2} M and the $[C]_0$ was 0.18 M. Figure 4 presents $^{31}P\{^1H\}$ FT NMR spectra recorded at −23 °C that were obtained for samples of reaction mixture taken at predetermined points in the hydrogenation. Figure 4 also contains −23 °C ^{31}P FT NMR spectra of 1.5×10^{-2} M I alone and 1.5×10^{-2} M I preequilibrated for 18 h with 0.10 M C, a concentration of C which corresponds to 40% reaction in the hydrogenation reactions. The 40% reaction point roughly corresponds to the completion of the induction period and the region of maximum reaction rate under these conditions. Although the recorded spectra in Figure 4 that are to be compared are not strictly identical with respect to experimental NMR parameters, the increase and eventual decrease in the concentration of VI is apparent in the reaction that was not preequilibrated and the concentration of VI does indeed reach a maximum comparable to that of the control experiment near 40% reaction. The preequilibrated reaction is seen to contain an initially high concentration of VI that steadily decreases throughout the run. Comparison of the 40% reaction sample from the hydrogenation solution with the 40% reaction control solution shows approximate agreement mitigated by instrumental differences. It may be concluded that the induction period and the apparent half-order rate dependence on both [C] and $[Rh]_t$ of a typical hydrogenation reaction are associated with the attainment and maintenance of

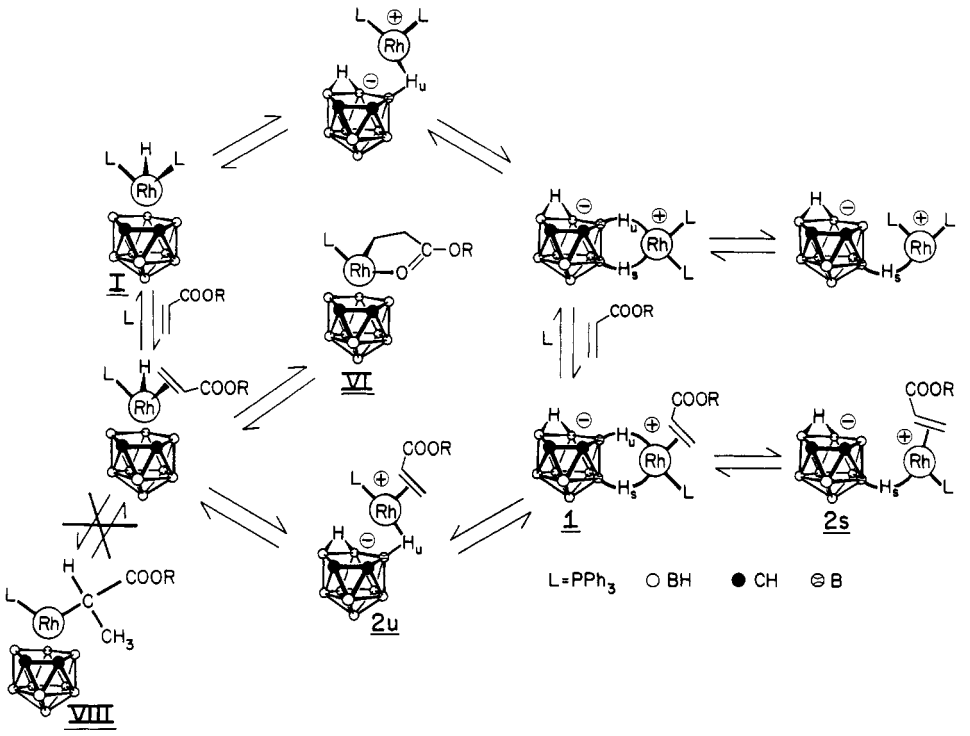

Figure 5. Possible equilibria derived from I and C showing interconversion of closo and exo-nido intermediates including proposed hydrogenation intermediates **1** and **2s**. Precursor III may involve itself in similar equilibria, thereby producing intermediates that are isomeric counterparts of **1**, **2s**, etc.

a steady-state concentration of VI, as pointed out above.

Discussion

***Closo–Exo-Nido* Tautomerism, Triphenylphosphine–Acrylate Interchange, and Acrylate Hydridometalation Equilibria.** Figure 5 depicts the array of equilibria in which I may conceivably participate in the presence of C or other acrylate esters. While only the fate of I is presented in Figure 5,other catalyst precursors such as II and III would be expected to generate similar sets of equilibria. The results presented above clearly demonstrate the importance of the hydridometalation of acrylate esters by the closo precursors I and III to produce VI and VII, respectively. The isomeric hydridometalation product VIII derived from I or its counterpart derived from III was not detected spectroscopically. In addition, the rapid formation and reversible decomposition of VIII would result in facile exchange of Rh–D with acrylate ester temminal methylene protons. Since only very slow Rh–D exchange was observed, species VIII appears to be unimportant.

The previously proposed mechanism[7a] of closo–exo-nido tautomerism is depicted in Figure 5 and is thought to proceed through exo-nido intermediates such as **2u** that contain a single hydride bridge connecting an L_2Rh^{1+} center (L = PPh_3) with an *unsaturated* BH_u vertex (hence subscript u). It was also earlier suggested[4] that intermediates such as **2u** play little or no direct role in catalytic hydrogenation (or related) mechanisms due to their propensity to isomerize to closo species through internal oxidative addition of Rh(1+) to the open face of the carborane ligand. On the other hand, intermediates such as **2s**, which are essentially identical with complexes exemplified by **2u** save for the presence of a bridging hydride which emmanates from a *saturated* BH_s vertex (hence subscript, s), are proposed as the reactive alkene-containing Rh(1+) species that activate H_2 or initiate alkene isomerization, etc (see Figure 6) at the outset of catalytic cycles. Both **2s** and **2u** would be expected to reversibly bind solvent at Rh to produce 16-electron species (**2s** in Figure 6) although 14-electron desolvated **2s** may be the reactive intermediate that undergoes oxidative addition with H_2. The common precursor of **2u** and **2s**, **1**, was not detected spectroscopically or by other means.

Figure 6 presents a proposed catalytic cycle that is in agreement with the experimental results reported above and closely related to the mechanism previously suggested[4] for the hydrogenation of A. As in the case of A hydrogenation, deuterium-labeling experiments have shown that B–H vertices of the rhodacarborane intermediates play no role in the mechanism. The Rh–H vertex present in I and III was similarly shown to be uninvolved in the hydrogenation of C. Thus, the exo-nido Rh(1+) species **1** remains as the initial Rh(1+) alkene intermediate in C hydrogenation.

The suggested mechanism for the hydrogenation of C is presented in Figure 6 and is essentially identical with the mechanism proposed for A and B hydrogenation.[4] However, the fact that D_2 reduction of C leads to a comparatively less random distribution of deuterium between recovered C and propionate product (60–80% 1-butyl propionate-d_2) than the corresponding deuterium distribution seen in A and B hydrogenation coupled with the near perfect fit of the experimental deuterium balance to $\Delta = 1.00$ (Table II) requires H_2 (D_2) activation to be rate determining and essentially irreversible. Deuterium scrambling into C reactant and the formation of 1-butyl propionate-d_0–d_4 is suggested to occur via the very rapid interconversions of species **4**, **5**, **6**, and **7** formed via species **3** that is generated by slow and rate-limiting D_2 activation. The appearance of small quantities of C-d_2 and 1-butyl propionate-d_4 demands that species **6**, as well as **5**, must be involved in the overall mechanism since **5** alone would exclusively produce C with a maximum of one D atom per molecule. Species **5** and **6** taken together would allow the exchange of up to three H atoms by deuterium. As a consequence of these observations the k_6 and k_7 reactions of Figure 6 are suggested as parallel routes to product from **5** and **6**, respectively. The elimination of 1-butyl propionate from **5** would involve a reversible scission of he C=O—Rh bond to generate a coordinatively unsaturated alkyl hydride (not shown) that would then decompose to products in a relatively slow step. In a similar fashion, **6** could proceed to products via the slow decomposition of a desolvated five-coordinate intermediate. The small inverse deuterium kinetic isotope effect, $(k'_{corr})_{H_2}/(k'_{corr})_{D_2} = 0.92$ at 0.58 atm of D_2, is not interpretable although it closely corresponds in magnitude to k_H/k_D values obtained in A reductions.

Kinetics and Mechanism. Assuming that the intermediate **1** in Figures 5 and 6 is in equilibrium with the catalyst precursor I and C after the establishment of steady-state concentrations of I, VI, and PPh_3 and that this equilibrium is rapid when compared

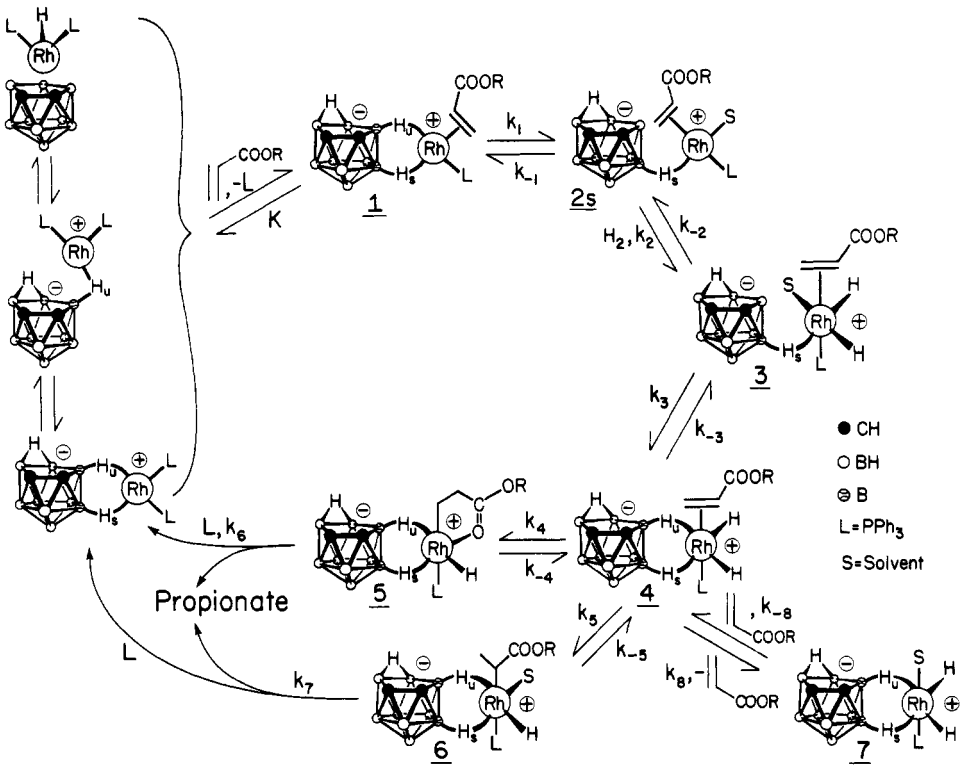

Figure 6. Proposed catalytic pathways for C hydrogenation using catalyst precursor I. Catalyst precursor III is thought to function through a completely analogous set of reactions.

to the rate of hydrogenation of C, it is possible to express the instantaneous concentration of **1** by eq 7. The equilibrium

$$[1] = \frac{K[(C)][(I)]}{[PPh_3]} \qquad (7)$$

constant K is composed of the several equilibrium constants associated with the equilibria displayed in Figure 5 that connect I with **1**. An identical situation would be expected if I were replaced by its counterpart III except for the magnitude of the corresponding K and the accompanying formation of VII rather than VI. The discussion below deals exclusively with I, but precursor III would be subject to the same general arguments.

The rate law described by eq 6 is identical with that obtained in A hydrogenation using both closo and exo-nido catalyst precursors.[4] Consequently, the scheme for C hydrogenation presented in Figure 6 is proposed by direct analogy to the corresponding scheme for A and B hydrogenation. As pointed out above, the form of the experimental rate equation does not distinguish the rate-determining step in either A or C hydrogenation except to say that the rate-determining step at low H_2 pressure is H_2 activation or a subsequent step and that PPh_3 and H_2 do not complete for reaction with a common intermediate.[4] If, as proposed here, H_2 activation (k_2 step) is slow and irreversible, then eq 8, which

$$\frac{-d[H_2]}{dt} = \frac{Kk_1k_2[I][C][H_2]}{[L]\{k_{-1} + k_2[H_2]\}} \qquad (8)$$

incorporates the [**1**] derived from eq 7, may be written in which $[I] = [I]_0 - [VI]$. Rearrangement of eq 8 allows its conversion to eq 6, which was determined from experimental data, giving $C = 1/Kk_1$ and $m = k_{-1}/Kk_1k_2$. Experimental values of C^I and C^{III} are 5×10^4 and 7×10^3 s, respectively, from which $Kk_1 = 2 \times 10^{-5}$ s^{-1} for I and 1.4×10^{-4} s^{-1} for III. The corresponding experimental evaluation of m^I and m^{III} gave 88 and 32 Ms, respectively. The Kk_1 values obtained[4] with I and III in the hydrogenation of A were 3.4×10^{-6} and 1.8×10^{-5} s^{-1}, respectively. Thus Kk_1 is greater for III than for I in both A and C hydrogenation, and the Kk_1 values are greater for both I and III in C hydrogenations than in A hydrogenations. The latter fact may reflect the stronger binding of C to Rh(1+) in *exo-nido*-**1** than is observed in the corresponding intermediate derived from A.

The rapid equilibration of species **5**, **6**, and **4** coupled with rapid external dissociative exchange of **4** with alkene suggests that collapse of the terminal alkyl hydride intermediates to propionate (k_6 and k_7 steps) are slowed to such an extent as to allow these interconversions to repeatedly occur. The previously discussed[4] weak electron donor properties of the $[\eta^2\text{-}nido\text{-}C_2B_9H_{12}]^-$ family of ligands may result in stabilization of dihydride as well as HRh^{III}(alkyl) intermediates.

Conclusions

The study reported here lends further support to the previously proposed scheme of alkene hydrogenation,[4] with an alternative identification of the rate-determining step, brought about through the use of *closo*-bis(triphenylphosphine)rhodacarboranes as catalyst precursors. In the present case, the hydrogenation reaction was complicated by the reversible hydridometalation of C with I or III. The importance of Rh(1+) and Rh(3+) exo-nido hydrogenation intermediates is apparent, and the icosahedral cluster structure[5] associated with both I and III does not directly support catalysis.

A later paper in this series will describe the mechanism of the novel catalytic hydrogenolysis of alkenyl acetates to produce alkene and acetic acid catalyzed by rhodacarboranes, a reaction which again suggests that decomposition of HRh^{III}(alkyl) species to alkane is slowed in rhodacarborane systems relative to alternative β-elimination reactions.

Experimental Section

General Methods. All reactions involving air-sensitive materials were performed[10] under deoxygenated argon in a standard vacuum line or in an efficient glovebox. NMR solvents were dried, degassed, and vacuum transferred into NMR tubes containing the solid samples at −196 °C and sealed in vacuo. ^1H and ^{31}P NMR spectra were recorded on a Bruker WP-200 spectrometer at 200.133 and 81.02 MHz, respectively. Proton chemical shifts are referenced to residual protons in the solvent. Phosphorus chemical shifts were determined as described elsewhere[11] with respect to 85% H_3PO_4. The ^{11}B NMR spectra were recorded at 126.7

(10) Shriver, D. F. "The Manipulation of Air-Sensitive Compounds"; McGraw-Hill: New York, 1969.

(11) Marder, T. B.; Baker, R. T.; Long, J. A.; Doi, J. A.; Hawthorne, M. F. *J. Am. Chem. Soc.* **1981**, *103*, 2988.

or 160.4 MHz. The lower frequency spectrometer was designed and built by Prof. Anet of this department, and the higher frequency spectrometer was a Bruker WM-500. Infrared spectra were obtained by using a Perkin-Elmer 137 or 521 instrument. Mass spectra were obtained at 70 eV by using a Perkin-Elmer Sigma 3/Kratos MS 25 system equipped with a J and W Scientific, Inc., SE 52 glass capillary column. Routine GLC analyses were performed by using a Varian 1700 or Hewlett-Packard 5880 instrument using either 10% Carbowax 20M on acid-washed Chromosorb P column, a 27% $AgNO_3$/37% Carbowax 600 on Chromosorb P column, or a J and W DB-1 capillary column.

Benzene and tetrahydrofuran were distilled from potassium metal, and ether was distilled from sodium–potassium alloy.

Materials. Benzene, tetrahydrofuran and diethyl ether (Mallinckrodt), triphenylphosphine, 1-butyl acrylate (stabilized), *p*-methoxyphenol, and sodium hydride (60% dispersion in mineral oil) (Alfa Products), argon, hydrogen (special purity 99.999%), and deuterium (Liquid Carbonic), activity I alumini (Merck), and hydroquinone were commercially available. *closo*-3,3-$(PPh_3)_2$-3-H-3,1,2-$RhC_2B_9H_{11}$ (I), *I-d*$_9$,[4] and I-*3-d*, *closo*-2,2-$(PPh_3)_2$-2-H-2,1,7-$RhC_2B_9H_{11}$,[5] (II), *closo*-2,2-$(PPh_3)_2$-2-H-2,1,12-$RhC_2B_9H_{11}$,[12] (III), *exo-nido*-$(PPh_3)_2$Rh-μ-7,8-$(CH_2)_3$-7,8-$C_2B_9H_{10}$,[6] (IV), [*nido*-7,8-$C_2B_9H_{12}$]$^-$,[13] [*nido*-7,9-$C_2B_9H_{12}$]$^-$,[13] [*nido*-2,9-$C_2B_9H_{12}$]$^-$,[11] and [*nido*-μ-7,8-$(CH)_3$-7,8-$C_2B_9H_{10}$]$^-$[14] were prepared by literature methods. Acrylate esters were passed through activity I alumina, freeze–pump–thawed over CaH_2 three times, and distilled in high vacuum immediately prior to use.

Determination of K_{VI} and K_{VII}. Weighed samples of I and III were transferred to 10-mm NMR tubes and attached to the vacuum line and the desired quantities of THF and C vacuum transferred to the NMR tube, and the tube was sealed off under vacuum. Sample tubes were equilibrated during a 24-h period at 41 °C. Integration of ^{31}P FT NMR spectra determined at that temperature provided the relative concentrations of the species required to calculate K_{VI} and K_{VII}. The equilibrium constants so obtained were reproducible over wide C concentrations ranges to within about ±10%; $K_{VI} \simeq 1 \times 10^{-3}$ and $K_{VII} \simeq 1 \times 10^{-2}$.

Exchange of I-*3-d* with C. Experiments that equilibrated 5.4×10^{-3} M I-*3-d* with 0.16 M C at 41 °C were conducted by using a previously described procedure[4] and Rh–H analytical method. An apparent first-order rate of Rh–D loss under these conditions was observed with $k = 1.4 \times 10^{-6}$ s^{-1}.

Catalysis of C Hydrogenation by Precursors I-*3-d* and I-*d*$_9$. Hydrogenation of C was carried out under normal kinetic conditions at 40.8 °C in separate experiments which employed I-*3-d*[5] and I-*d*$_9$[4] as catalyst precursors. Analyses of recovered catalyst precursor samples by previously described methods[4] proved that I-*d*$_9$ gave no detectable exchange of BD with H_2 after 90 hydrogenation turnovers. After seven such turnovers, I-*3-d* retained 84% of its original (95%) isotopic purity, and in a second experiment it retained 74% of its original RhD after 11 turnovers.

Kinetic Procedure for C Hydrogenation. Precisely the same procedure and apparatus was employed in C hydrogenation as was employed in the previously described hydrogenation studies[4] which employed A as a substrate. Table I provides reactant concentrations and other details. Instantaneous rate data obtained from the automatic hydrogen titrator was reduced to useful form through application of the integrated half-order equation by means of a locally written Fortran program.

Reduction of C with D_2 Using Catalyst Precursor I. Using the previously decribed procedure and flow apparatus[4] C was reduced with D_2 in the presence of I and samples removed at intervals for GC/MS analyses. Table II reports these results.

Demonstration of the Reversible Formation of VI during the Hydrogenation of C with I. As described above (Results), hydrogenation reactions were carried out by using the usual kinetic procedure and reactant solutions that were preequilibrated for 18 h before the admission of H_2 and identical reactant solutions that were not preequilibrated. In both cases, 2 mL aliquots of reaction solution was intermittently withdrawn and chilled to −23 °C and the ^{31}P FT NMR spectrum recorded. Control solutions were prepared and examined in a similar manner. Results are presented in Figure 4.

Acknowledgment. We with to thank the National Science Foundation for generous support of this research under Grant CHE83-00590 and its predecessors. We also thank the National Science Foundation for the purchase of the Bruker FTNMR spectrometer under Grant CHE77-05926. We also acknowledge the use of the Southern California Regional NMR Facility supported by the National Science Foundation Grant No. CHE79-16324.

Registry No. I, 53687-46-0; I-*3-d*, 82808-04-6; I-*d*$_9$, 89462-06-6; II, 53754-45-3; III, 76287-18-8; IV, 89437-71-8; VI, 92694-67-2; VII, 92694-68-3; butyl acrylate, 141-32-2; butyl propionate, 590-01-2.

(12) Busby, D. C.; Hawthorne, M. F. *Inorg. Chem.* **1982**, *21*, 4101.
(13) Hawthorne, M. F.; Young, D. C.; Garrett, P. M.; Owen, D. A.; Schwerin, S. G.; Tebbe, F. N.; Wegner, P. A. *J. Am. Chem. Soc.* **1968**, *90*, 862.
(14) Paxson, T. E.; Kaloustian, M. K.; Tom, G. M.; Wiersema, R. J.; Hawthorne, M. F. *J. Am. Chem. Soc.* **1972**, *94*, 4882.